THE JOURNAL OF PHYSICAL CHEMISTRY C

Article

Cite This: J. Phys. Chem. C 2019, 123, 26769−26776

pubs.acs.org/JPCC

Charge Transfer during the Dissociation of H_2 and the Charge State of H Atoms in Liquid Gallium

Dulce C. Camacho-Mojica,[†] Benjamin Cunning,[†] Shahana Chatterjee,[†] Sunghwan Jin,[†] Feng Ding,[†,‡] Jean-Christophe Charlier,[⊥] and Rodney S. Ruoff*[,†,‡,§,∥]

[†]Center for Multidimensional Carbon Materials (CMCM), Institute for Basic Science (IBS), Ulsan 44919, Republic of Korea

[§]Department of Chemistry, [‡]School of Materials Science and Engineering, and [∥]School of Energy and Chemical Engineering, Ulsan National Institute of Science and Technology (UNIST), Ulsan 44919, Republic of Korea

[⊥]Institute of Condensed Matter and Nanosciences (IMCN), Université catholique de Louvain (UCLouvain), Louvain-la-Neuve, Belgium

Supporting Information

ABSTRACT: *Ab initio* calculations have been performed on the liquid gallium−hydrogen system at 100 °C. Gallium was found to interact with both free hydrogen atoms and H_2, transferring charge in the process. First-principles computer modeling showed that the dissociation of H_2 is a consequence of charge transfer in liquid gallium−hydrogen systems, even at low temperature. Once negatively charged, hydrogen atoms interact with each other and are stabilized by positively charged gallium atoms inducing local atomic arrangements analogous to parts of the digallane molecule.

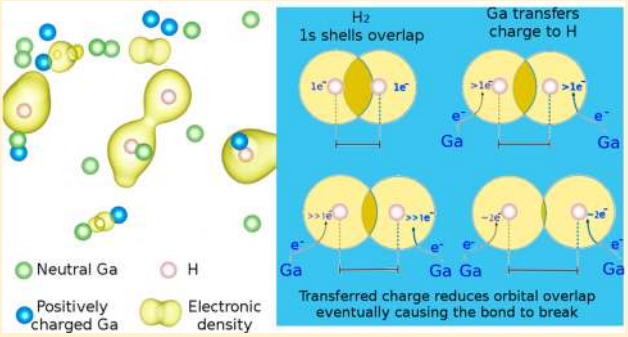

1. INTRODUCTION

Liquid metals, defined as metals and alloys with melting point up to 330 °C, including gallium as one of the most widely explored, are now emerging also in nanotechnology.[1] They are considered for use in stretchable electronics,[2] energy storage,[3] catalysis,[4] and chemical sensing.[5,6] Recent studies have emphasized using the molten metal as a solvent for reactions.[7−9] Among liquid metals, gallium is of special interest, as it has a near room temperature melting point (29.76 °C), a wide liquid-state temperature range (boiling point at 2204 °C), and low toxicity[10] and is capable of forming alloys with In and Sn[11] that have eutectic (melting) temperatures below room temperature. Recent reports of gallium and its alloys being used as reaction solvents for dispersing catalysts,[12,13] or as catalysts in their own right, are bringing renewed attention to gallium and its eutectics.

To the best of our knowledge, there are only a few theoretical studies of the electronic density in liquid metal systems.[10,14,15] For example, methane was (experimentally) reported to decompose in a liquid (bubble column) that consisted of a dissociation catalyst (Ni) dispersed in a liquid metal (Bi). This process was reported to generate only hydrogen (H_2) gas and graphitic carbon.[15] Density functional theory (DFT) calculations were also performed reporting that a charge transfer occurs from a liquid metal (Sn, not Bi) solvent to a dissociation catalyst (Pt, not Ni), and the authors correlated this amount of charge transfer to the catalytic activity.[15]

In another report, a 270-μm thick liquid gallium membrane was sandwiched between porous SiC frits to examine its feasibility in fuel cell applications.[16] H_2(g) and He(g) were introduced upstream of the membrane, and only hydrogen diffused through the liquid gallium with a permeance significantly higher than in Pd (as measured downstream, as the H_2 molecule; helium was "rejected" by the liquid gallium layer). A follow-up theoretical work investigated the same system using Pauling Bond Valence potential modeling, and the authors thereby suggested that H_2 was dissociating in the liquid gallium.[17] Although the semiclassical simulations could reproduce their experimental observations, the limitation of their chosen modeling technique did not allow the authors to consider either charge transfer or the liquid state in their system. Furthermore, to the best of our knowledge, there has not been any experimental proof of dissociation of molecular hydrogen in liquid gallium.

Thus, we have chosen to study by *ab initio* molecular dynamics simulations of hydrogen (atoms and molecules) in liquid gallium. We postulated that H might be negatively charged, as frequently observed in metal hydrides.

Received: July 17, 2019
Revised: September 25, 2019
Published: October 25, 2019

DOI: 10.1021/acs.jpcc.9b06779
J. Phys. Chem. C 2019, 123, 26769−26776

2. COMPUTATIONAL DETAILS

Electronic density calculations (Bader charge analysis) were performed within the density functional theory (DFT) framework.[18,19] The generalized gradient approximation (GGA) with Perdew−Burke−Ernezerhof (PBE) parametrization was selected for the exchange-correlation functional as implemented in the Vienna Ab initio Simulation Package (VASP).[20,21] The projected augmented wave (PAW) method was used to describe the interaction between valence electrons and ion cores. A *k*-point grid of 4 × 4 × 1 was used to sample the Brillouin zone of the supercell related to the liquid gallium model, while only the Γ-point was used for the molecules (digallane, diborane, etc.) also studied here. The atomic structures were optimized until the forces on each atom were less than 0.01 eV/Å with an energy convergence criterion of 10^{-5} eV.

Ab initio molecular dynamics (MD) simulations with similar parameters as the ones used for ground state calculations and a *k*-point grid of 5 × 5 × 1 were used to sample the Brillouin zone of the supercell (see Figure S1 for the convergence test) as implemented in the VASP code (which applies the Born−Oppenheimer approximation). A canonical ensemble (NVT) with a Nosé−Hoover thermostat set to 373 K was used with a time step of 2 fs and a total trajectory time of 4,742 fs (i.e., 4.742 ps). Liquid gallium was modeled with 80 Ga atoms (in a slab with a height of ∼11 Å) that were previously annealed in another MD simulation for 10 ps at 373 K. The simulation box dimensions were 10.50 × 13.50 × 30.00 Å, with a vacuum region (∼19 Å) along the *z*-direction between two surfaces. Periodic boundary conditions were applied in the *x* and *y* directions (see Figure S2).

The electronic density of the liquid gallium−hydrogen atom system during the MD trajectory was calculated by extracting the atomic positions every 100 fs from the MD trajectory and performing a single point (no relaxation steps) calculation as described above; the "Bader Charge Analysis" code was used.[22,23]

Since a NVT ensemble is used, a vapor phase could potentially appear above the surface of the liquid. However, the vapor pressure of gallium is 2.55 × 10^{-20} mbar at 373 K (extremely low) as compared to other liquid metals (e.g., 0.374 mbar, ref 24, for Hg at 373 K). Consequently, the present atomistic model including a vacuum region is very likely adequate to simulate liquid gallium.

3. RESULTS AND DISCUSSION

3.1. Calculated Molecular Structure and Electronic Charge Distribution of Digallane, Diborane, In_2H_6, Al_2H_6, and Tl_2H_6 Molecules, and Radial Distribution Functions (RDFs) of Pure Liquid Gallium and Liquid Gallium with Embedded H Atoms. Group 13 is the first periodic group containing post-transition metals that are electropositive, i.e., tending to lose electrons rather than gaining them during chemical reactions. When reacting with hydrogen, these group 13 elements form hydrides,[25,26] such as diborane[27] and digallane[28,29] that are experimentally known. Both diborane and digallane have similarities in their electronic density distribution (see Figure S3), and the uniqueness of the bonding in these molecules has attracted significant investigation.[30]

In the digallane molecule (see Figure 1), the electronic density in Figure 1(a,b) shows that hydrogens are bonded to

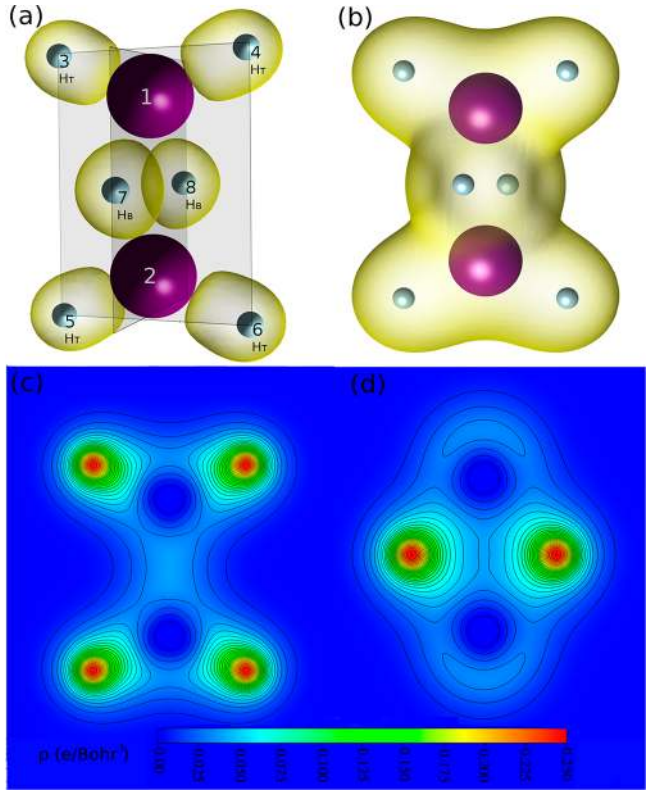

Figure 1. Electronic charge distribution in the digallane molecule (Ga_2H_6). (a) Schematic of digallane molecule with an electron density isosurface at 0.042 e/Bohr^3. Atoms 1 and 2 are Ga, while 3 to 8 are H. H_B and H_T indicate the bridge and terminal atoms of hydrogen, respectively. Atom numbers labeled in this figure correspond to the atom numbers in Table S1, with atoms 1 and 2 replaced by the appropriate group 13 element. Electron density isosurface of digallane at 0.042 e/Bohr^3. (b) Electron density isosurface of digallane at 0.012 e/Bohr^3. (c) Contour maps of valence electron density in the plane that contains atoms 1 to 6 and (d) atoms 1, 2, 7, and 8, which show that Ga atoms transfer charge to the H atoms. Contour lines are at intervals of 0.01 au. Electronic charge distribution for analog molecules can be found in Figure S3.

Ga in two ways; (i) in terminal bonds (H_T, two-center), where a polar bond forms between one hydrogen and one gallium atom (see Figure 1(c)), and (ii) in bridge bonds (H_B, three-center) where two gallium atoms are bridged by one hydrogen (Ga−H−Ga). Digallane (as well as diborane) thus have curved double bridge bonds in which an H atom bridges two Ga atoms "above and below" (see Figure 1(d)). When a Bader analysis of the electronic density was performed, a chemical bond (path of maximum electronic density joining two nuclei) was found between the two bridge hydrogens even though each H has a partial negative charge (see Table S1). This bond between the bridging (negatively charged) hydrogens is enabled by the positive charge present in the two Ga atoms.

Some preliminary studies were first undertaken regarding interatomic distances. For diborane, the DFT equilibrium B−H_T and B−H_B distances are 1.197 and 1.322 Å, respectively, which can be compared to (B−H_T = 1.19 Å and B−H_B = 1.32 Å) obtained from electron diffraction and high resolution infrared and Raman spectroscopy of gaseous diborane.[31] For digallane the DFT equilibrium Ga−H_T and Ga−H_B distances are 1.562 and 1.769 Å, respectively, which can be compared to (Ga−H_T = 1.550 Å and B−H_B= 1.723 Å) obtained from gas-

DOI: 10.1021/acs.jpcc.9b06779
J. Phys. Chem. C 2019, 123, 26769−26776

phase electron diffraction and infrared spectroscopy of gaseous diborane.[32] We next compared the DFT calculated equilibrium bond lengths of digallane (at 0 K) to the radial distribution function (RDF) obtained at 373 K MD for digallane (further discussions about the RDF are provided in Note S2). This comparison (Figure S4) shows that the calculated equilibrium bond distances of digallane (at 0 K) closely match the highest probabilities in that RDF. The calculated structures and Bader charges of In_2H_6, Al_2H_6, and Tl_2H_6 are described in Note S1, Table S1, and Figure S3.

To test whether the present simulation accurately models the liquid state of gallium, the RDF of various Ga atom−Ga atom pairs have been extracted from the MD run (Figure 2a).

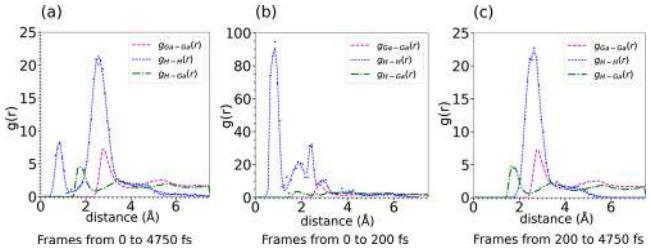

Figure 2. Radial distribution functions corresponding to different time frames of the MD run. (a) RDF from frames taken from 0 to 4750 fs. The first peak in the $g_{H-H}(r)$ RDF corresponds to the H_2 molecule (before it dissociates). The second peak at 2.75 Å indicates an interaction between two negatively charged H atoms. (b) RDF of first 200 fs only. (c) RDF taken from frames from 0 to 4750 fs. Notice that in (c) the peak centered at around 0.86 Å in $g_{H-H}(r)$ is not present, while in (b) the tallest peak is the one centered at 0.86 Å.

The RDF for these Ga−Ga pairs is in quite good agreement with the experimental RDF of liquid gallium at 373 K measured by X-ray absorption fine structure[33](see Figure S5). Thus, with confidence that liquid gallium is being well modeled, we turned next to studying the system with four H atoms dissolved in liquid gallium (containing 80 Ga atoms).

Eighty atoms of gallium were "annealed" using the quantum MD technique at a temperature of 373 K for 10 ps using a Nosé−Hoover thermostat. The linear behavior of the mean square displacement as a function of time in Figure S6 prove that the metal is in liquid state. Periodic boundary conditions in three dimensions created an infinite slab of liquid gallium since a vacuum region of 19 Å was included in the super cell between the liquid surfaces to ensure they did not interact (see Figure S1). To simulate a "cavity" in Ga, some adjacent Ga atoms were relocated from an interior region to the liquid surface then four H atoms were added within this less crowded region. Two of the H atoms (H1 and H2) immediately formed an H_2 molecule, while the other two H atoms (H3 and H4) were isolated (unbound hydrogen). The MD simulation ran for 4.74 ps with 2 fs time steps. Further details are available in the Computational Details section above. It was found that the newly formed H_2 molecule remained in the cavity for almost the first 200 fs of the run (see Video S1). At about 170 fs this H_2 molecule began to dissociate (it fully dissociates just prior to 200 fs), and after 200 fs, the cavity shrank and disappeared. The two H atoms (H1 and H2) moved in opposite directions. In this particular trajectory, H1 traveled to the far liquid surface within the first picosecond of the trajectory, while the other H atoms (H2, H3, and H4) remained close to the surface nearest the original cavity.

The shape of the H−H RDF for the entire trajectory (Figure 2a) exhibits an unusual feature in that it has two sharp peaks of different radii. The first radial peak corresponds to a R_0 at 0.5 Å, which is exactly the hard sphere radius of neutral hydrogen[34] and thus is attributed to the H_2 molecule (see Note S2 for a definition of R_0). The second H−H radial peak is atypical for an RDF as it has a larger intensity than the first peak, indicating that another H−H interaction is also occurring. As the first radial peak is likely due to the H_2 molecule, the RDF spectra were separated before (Figure 2b) and after (Figure 2c) the hydrogen dissociation event (~200 fs). As the RDF before H_2 dissociation (Figure 2b) has the highest probability for occurring at an H−H distance of around 0.86 Å and only one H−H interaction is observed in the RDF after dissociation (Figure 2c), this result clearly indicates that the second radial peak in Figure 2a cannot be related to the H_2 molecule. However, when the RDF of the MD Ga−H system is compared to the DFT equilibrium distances in digallane (Figure S7), the maximum probability of H−H pairs in the RDF is found to match the H−H equilibrium distances in digallane. Consequently, the nature of the second hydrogen interaction in the MD run could be similar or analogous to the digallane molecule. As hydrogen atoms in digallane exhibit a partial negative charge, the H atoms were thought to perhaps also be negatively charged to account for the increase in the R_0

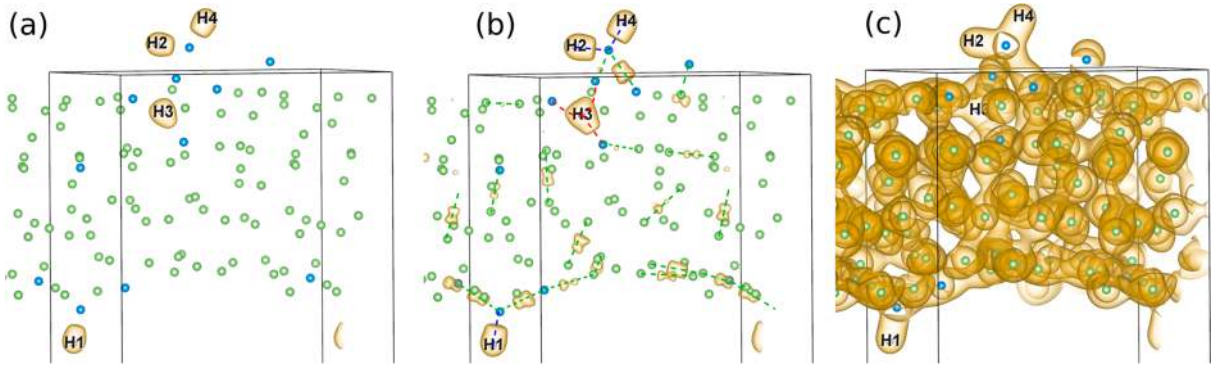

Figure 3. Electron densities of the Ga−H model for a configuration of the MD run at 4400 fs. (a) Isosurfaces at 0.05 e−/Bohr^3 enclose a small volume only around each of the H atoms. (b) Isosurfaces at 0.04 e−/Bohr^3 show the electronic density shared in Ga dimers and the H electronic density "pointing" toward neighboring gallium, thus forming bonds similar to the bonds in the molecule digallane. (c) Isosurfaces at 0.03 e−/Bohr^3 depict electron delocalization throughout the liquid gallium.

DOI: 10.1021/acs.jpcc.9b06779
J. Phys. Chem. C 2019, 123, 26769−26776

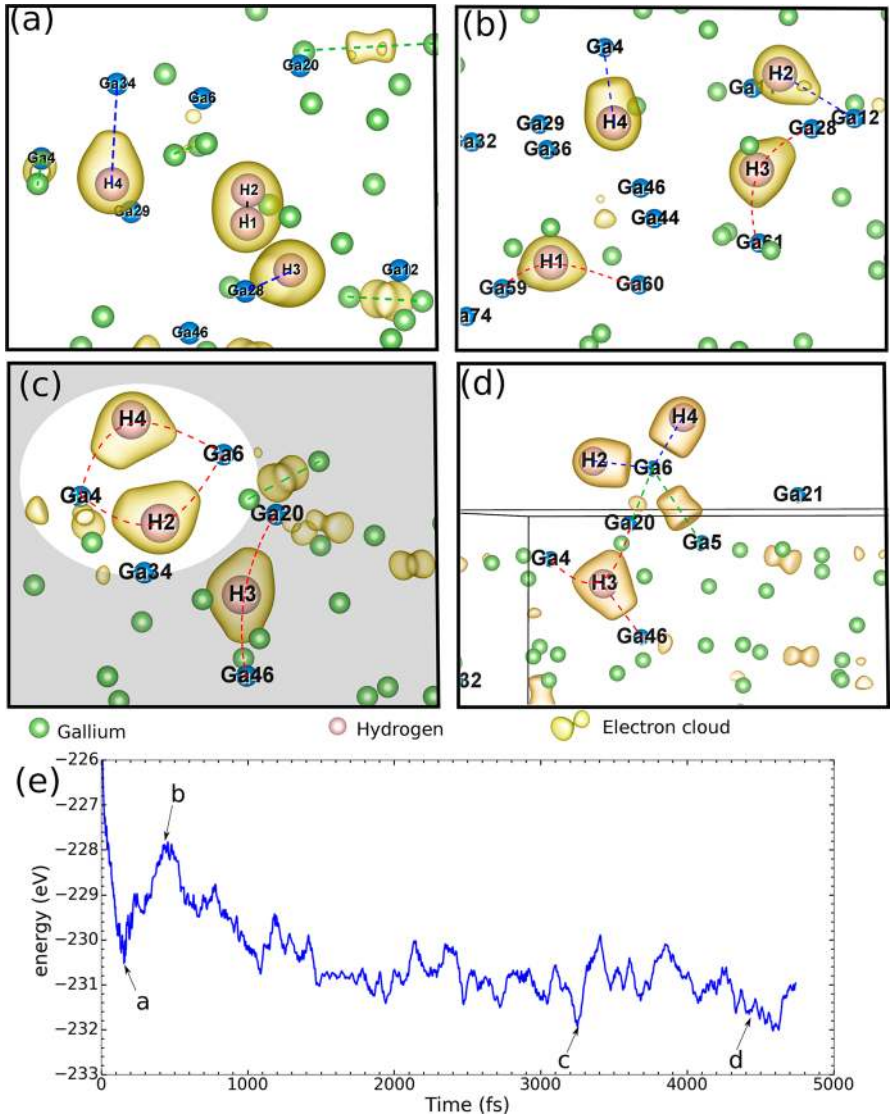

Figure 4. Electronic densities (isosurfaces at 0.04 e−/Bohr^3) for different atomic configurations extracted from the MD run: (a) 160 fs, before the H_2 molecule dissociation; (b) 400 fs, after H_2 dissociation, and before H1 reaches the lower surface; (c) 3300 fs, showing a double bridge formation by H2 and H4 between Ga4 and Ga6 (analogous to digallane); (d) 4400 fs, shows two terminal bonds between Ga6 and the two hydrogens H2 and H4 leading to a protrusion out of the liquid surface. (e) Ion electron energy of the Ga−H liquid model as a function of time. The labels (a−d) point out the energy of the four atomic configurations of the MD run used to investigate the corresponding electronic densities in (a−d).

to 0.9 Å (see discussion on the electronic charge distribution, below).

Because of the difficulty in acquiring experimental data for the hard sphere radius of negatively charged hydrogen, we have compared the predicted radius to the isoelectronic Li^+. By way of comparison, the isoelectronic Na^+ and F^- have ionic radii of 1.16 and 1.19 Å, respectively.[35] As Li^+ has an ionic radius of 0.90 Å,[35] we should expect an equal or slightly larger radius for a negatively charged H atom. Section 3.2 discusses how the Bader charge analysis also suggests the presence of negatively charged H atoms in the liquid gallium.

3.2. Liquid Gallium System with Four Hydrogen Atoms: Electronic Charge Distribution among the Atoms. Given the electronic charge distribution in the digallane molecule, we were inspired to calculate the electronic density distribution around the H and Ga atoms within the DFT framework in the liquid gallium system. The electronic density of the liquid gallium−hydrogen system was obtained using the atomic positions extracted from the 373 K ab initio molecular dynamic simulations. These atomic positions allow partitioning the charge to the different atoms according to the conventional Bader charge analysis technique (but calculated at 0 K, as is standard for the Bader charge analysis). Three representative isosurfaces of the resulting electron distribution are shown (see Figure 3) that highlight different electronic interactions present in this system. In Figure 3a, the isosurface of the electronic density at 0.05 e−/Bohr^3 encloses only the H nuclei. In Figure 3b, the isosurface at 0.04 e−/Bohr^3 reveals two types of bonds: (i) polar Ga−H bonds indicated by the electronic cloud around H that "points" in the direction of its first-neighbor Ga atom, and (ii) neutral and covalent Ga−Ga dimers (which are indicated in Figure 3b by the dotted lines that connect neighboring Ga atoms). Furthermore, while Ga−Ga dimers have been calculated to be present in the absence of hydrogen,[36] our MD simulations of both the pure liquid gallium and the liquid gallium containing the H atoms show that their formation is also catalyzed by hydrogen. In Figure 3c, the isosurface at 0.03 e−/Bohr^3 shows that delocalized orbitals

DOI: 10.1021/acs.jpcc.9b06779
J. Phys. Chem. C 2019, 123, 26769−26776

corresponding to metallic bonding are present throughout the liquid. This metallic behavior is similar to that calculated for pure liquid gallium.

The ion core (for gallium, the 31 protons and 28 core electrons)−electron (the 3 valence electrons) energy of the Ga−H liquid system as a function of time and various snapshots of the electronic density (at 0.04 e−/Bohr^3) for different atomic configurations during the MD run are shown in Figure 4. Figure 4a highlights the beginning of the H_2 dissociation process and corresponds to the first local energy minimum indicated in Figure 4e; the isosurface revealed that electronic density is shared between H1 and H2, indicating they are still bonded (black dashed line, Figure 4a). Bridge bonds similar to those seen in the digallane molecule are also visible (red dashed lines). In Figure 4b, the H_2 dissociation process has just ended corresponding to the largest local energy maxima (see Figure 4e). Note that all four H atoms have formed bonds with gallium; both terminal (Ga4−H4) and bridge-bonds (Ga59−H1−Ga60) are observed. In Figure 4c, a double hydrogen bridge (Ga4−H4−H2−Ga6) that has an orbital shape almost identical to the double bridge in the center of the digallane molecule (see Figure 1a,d) is observed. This configuration corresponds very closely to a local energy minimum obtained later in the MD run (see Figure 4e) thus suggesting a particular stability for this double-bridge atomic structure. Finally, in Figure 4d, terminal bonds (H2−Ga6, H4−Ga6) analogous to the terminal bonds in the digallane molecule are observed, persisting until the next local energy minima at 4.6 ps (Figure S18).

The H_T−Ga−H_T atomic structure was observed to "protrude" from the liquid surface for a duration of ∼500 fs. Although an H_2 desorption event has not been observed during the MD run (perhaps because of the limited MD time and/or the small number of hydrogen atoms in the model), this protrusion may provide a mechanism for H_2 reassociation and desorption through metastable structures such as GaH_3. The possible generation of H_2 at the surface should be the topic of future modeling studies.

After analyzing the electronic density of the system during the MD run, Bader charges were calculated for all atoms in the system every 100 fs (Tables S2−11). The amount of charge on Ga atoms was found to strongly depend on the number of interactions with hydrogen atoms. As an example, the charges of three selected Ga atoms during the course of the MD run are shown in Figure 5a. Ga54 did not interact with any H atoms throughout the whole MD run and its charge remained almost neutral. Ga74 was located at the farthest surface from the cavity where it formed a persistent H_T bond with H1 around ∼1 ps. At that specific surface, only one H atom was present (H1). Hence, no other interactions with H atoms were possible. The charge on Ga74 remained around +0.5e after bond formation. The Ga6 that was located near the surface had three H atoms in its vicinity. During the course of the MD run, the charge on this Ga atom varied depending if it was interacting with one, two, or three H atoms

As mentioned, the four H atoms were located inside the cavity in the liquid surrounded by gallium at the beginning of the MD run. As a result, they could interact with many Ga atoms simultaneously gaining negative charge from each interaction and filling their 1s orbital, as highlighted in Figure 4b. As the MD simulation progresses, all of the H atoms eventually move to the liquid surface. For geometric reasons, the number of possible interactions with Ga is limited at the

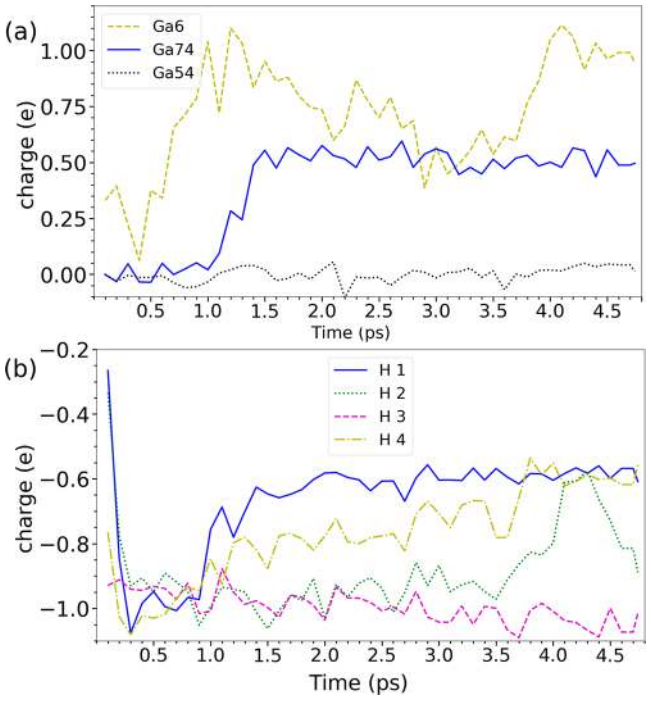

Figure 5. Bader atomic charges estimated for (a) Ga and (b) H atoms along the whole MD simulation. Ga atoms that are in close proximity with hydrogen acquire significant positive charge (i.e., Ga6 & Ga74). Some Ga atoms can have up to 3 first-nearest neighbors Ga atoms (e.g., Ga6, see Tables S2 and S4) resulting in charges exceeding +1.00 e. Regarding H atoms, at the beginning of MD run, H1 and H2 are present as an H_2 molecule and are almost unchanged. However, as the MD simulation progresses the atomic charge on each H atom becomes more negative as H_2 dissociates. H atoms may exhibit charge values more negative than −1.00 e when they are inside the liquid gallium and bonded to more than one Ga atom. When the H atoms reach the surface and have only one Ga neighbor, and charge stabilizes to a value close to −0.60 e. Full details of the charges of every atom during the MD trajectory can be found in the Supporting Information (Tables S2−11).

surfaces, and it was found that the H atoms then had smaller negative charges. Figure 5b displays the charge of the four H atoms obtained during the whole MD run. In the case of H1, it was the first to reach the liquid surface to form a stable H_T bond (Ga74). Since H1 did not form any additional interactions with other Ga atoms (see Figure 3), its charge stabilized at −0.60 e. Such a negative value is more negative than −0.29 e, the charge estimated for the terminal hydrogens in digallane (see Table S1). However, since the gallium-rich (liquid gallium) system is metallic, small amounts of charge were additionally transferred from non-nearest neighbor gallium atoms, thus increasing the H1 charge. This additional charge transfer from other Ga atoms also explains why the hydrogen charge (−0.60 e) is slightly higher in magnitude than the charge on the Ga (+0.50 e) directly involved in the terminal bond.

During the MD run, H3 remained below the liquid surface, which is why it had a charge around −1.00 e and, in some instances, even exceeded this value. From 1 ps onward, H2 and H4 share at least one nearest-neighbor Ga atom. The hydrogen closer to the surface always exhibits the lower charge. In Figure 4c (MD run, 3.4 ps) both H2 and H4 share two nearest-neighbor Ga atoms in a double bridge bond, but H4 (being closer to the surface) has a smaller charge. At ∼4.2 ps when

DOI: 10.1021/acs.jpcc.9b06779
J. Phys. Chem. C 2019, 123, 26769−26776

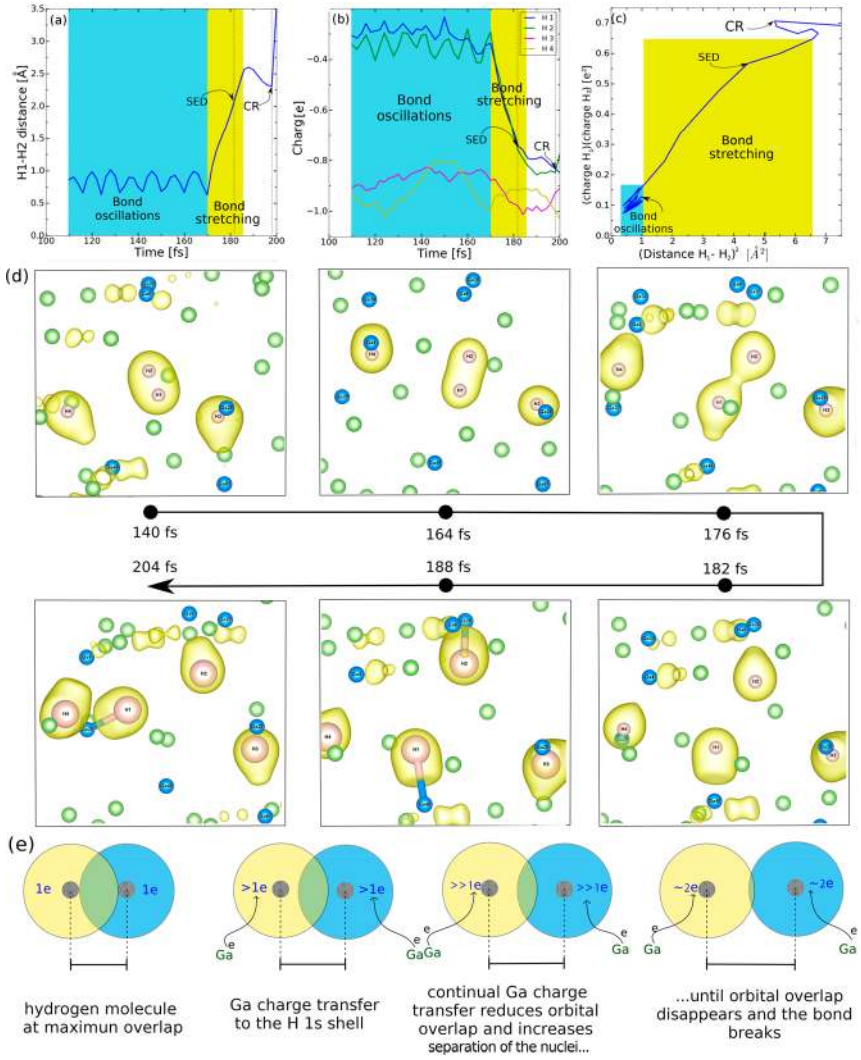

Figure 6. How the H_2 molecule dissociated during this trajectory in liquid Ga. (a) Distance between H1 and H2 (initially present as an H_2 molecule) as a function of time. Note the "bond oscillations" (blue region) followed by a "bond stretching zone" (yellow region). At 182 fs, a separation of the electronic density between the two H atoms (SED, at 0.05 e-/Borh^3) after which the bond breaks and the H1 and H2 atoms separate due to Coulombic repulsion (CR). (b) Charge on H1 and H2 as a function of time. The magnitude of the negative charge of H1 and H2 significantly increases during the bond stretching. After SED, the charges differ. (c) Product of the charges of H1 and H2 plotted against the square of the distance between them. The slope of this plot is proportional to the bonding force. (d) Electronic density snapshots at 0.04 e−/Bohr^3 during the dissociation process. (e) Schematic diagram explaining how charge transfer to the H_2 molecule results in bond stretching and then breaking.

both H2 and H4 are located at the liquid surface forming H_T bonds with Ga6, their charges are found to be almost identical (−0.60 e). Note that the charge of Ga6 (+1.00 e) at 4.1 ps with two H_T bonds is twice the charge of Ga74 (+0.50 e) that only forms one H_T bond.

3.3. Mechanism of Dissociation of the H_2 Molecule. In order to more deeply investigate the dissociation process of the H_2 molecule that occurred at the beginning of the MD run, Bader charges were estimated on each atom every 2 fs (full tables can be found in Tables S13−21) during the time window from 110 to 200 fs. The H−H bond length (Figure 6a) and H charge (Figure 6b) are displayed as a function of the MD time. At the beginning of the MD run the H_2 bond length oscillates as the molecular undergoes its (fundamental mode) "stretching" vibration (blue regions in Figure 6a−c). When the H−H separation is largest, the Ga atoms at the inner surface of the cavity interact with the approaching H, and in this trajectory, this is Ga6 and Ga20 interacting with atom H2 (Figure 6d 140 fs; please note that H2 is an atom, not the H_2 molecule); Ga6 and Ga20 transfer charge to H2, which is subsequently distributed in the H_2 molecule. This process repeats during each oscillation, slightly increasing the charge in the molecule.

In this particular trajectory, Ga46 exchanged charge with H4 (not a part of the H_2 molecule, but close to it). At 164 fs, this partially (positively) charged Ga46 moved toward the H_2 molecule, likely through Coulombic attraction, and it was found that charge was rapidly transferred from the three Ga atoms (Ga46, Ga6, and Ga20) to the hydrogen molecule. Ga20 is on the other side of the H_2 molecule than Ga46 and Ga6, and all 3 Ga atoms are essentially aligned with the stretching vibration (see yellow region in Figure 6a). Notice, in Figure 6b, that during the stretching of the H_2 molecule there is also a transfer of charge. This persistent charge transfer progressively fills the H 1s orbital and thus progressively weakens the bond. At 182 fs, the orbital overlap of H_2 has decreased to the point we see a separation in the electronic

DOI: 10.1021/acs.jpcc.9b06779
J. Phys. Chem. C 2019, 123, 26769−26776

density ("SED") at 0.04 e−/Bohr^3 (Figure 6d, 182 fs, and shown in more detail in Figure S19).

Figure 6c shows the product of the charges on atoms H1 and H2 (the atoms in the H_2 molecule) versus the square of the distance between them (the slope of this plot is proportional to the bonding force). We observed that the bonding force is constant during bond oscillation and stretching until the SED is reached. Due to the small orbital overlap and hence low probability for charge transfer in the H_2 molecule, the charges on H1 and H2 (that had been essentially equal up to that point during the final bond stretch event) differed from this point (i.e., the SED) onward. Even though there is no longer a molecular interaction, we still observed a weak interaction (visible in the isosurface at 0.012 e−/Bohr^3, Figure S19d) that was subject to thermal oscillations (Figure 6d, 188 fs). During the oscillation, the charge increased further reducing the orbital overlap until the bond broke. Note that the product of the charges on the H1 and H2 atoms (y axis of Figure 5c) is less than 1, thus the valence shells are not filled. Despite this, the interaction was weak enough that the bond broke. At this point, the 1s electrons no longer shared the same orbital and the H1 and H2 atoms experienced Coulombic repulsion (Figure 6d, 204 fs). As this simulation was performed at a low temperature (373 K), our result demonstrates that hydrogen dissociation in liquid gallium at this temperature is due to the transfer of charge and not a thermally activated process.

4. CONCLUSIONS

In this work, *ab initio* molecular dynamics simulations were used to investigate the liquid gallium system with solvated H atoms and an H_2 molecule. First, digallane and diborane were modeled and experimental bond distances closely agreed with the calculated values; Bader charges for Ga, H and B, H were also calculated for these two molecules, and each of the six H atoms in each molecule were found to be negatively charged (Al_2H_6, In_2H_6, and Tl_2H_6 molecules were also calculated). An 80-atom slab of liquid gallium was created, and MD simulations at 373 K closely matched the experimental radial distribution function (RDF) for pure gallium (also obtained at 373 K), validating the computational approach for the liquid gallium slab. Four H atoms were then added to the liquid gallium slab, and MD trajectories were obtained that allowed detailed study of atomic configurations of H and neighboring Ga atoms; it was thereby learned that the bonding configurations between H and Ga often "closely mimicked" those in digallane. Two of the H atoms immediately formed an H_2 molecule, and as the trajectory progressed, this molecule eventually dissociated. It was possible to "track" the progressive (negative) charging of this H_2 molecule while it vibrated in the liquid gallium; it became more and more negatively charged from charge transfer from nearby Ga atoms, and its dissociation was a result of the accumulating negative charge reaching a critical value. This charge transfer "capability" of liquid gallium opens its potential use as a dissociation catalyst operating even at very low temperatures.

Thus, liquid gallium readily donates its electrons (at least, per the Bader charge analysis), here to H atoms or H_2 molecules, and local Ga−H bonding configurations look like "parts" of the digallane molecule. From our calculations of the Bader charges on Al_2H_6, In_2H_6, and Tl_2H_6 described in Note S1, Table S1, and Figure S3, it seems reasonably likely that liquid aluminum and liquid indium could drive dissociation of H_2 by charge transfer and that local M−H bonding configurations might look like parts of Al_2H_6 and In_2H_6 molecules, as well. Thus, gallium, and also aluminum and indium, and perhaps other liquid metals, could drive the dissociation of other types of molecules containing elements such as those with nearly filled valence shells (e.g., halogens)

■ ASSOCIATED CONTENT

Supporting Information

The Supporting Information is available free of charge on the ACS Publications website at DOI: 10.1021/acs.jpcc.9b06779.

Computational details; digallane molecule (and group 13 analogs), liquid Ga, and liquid Ga-hydrogen systems; electronic density distributions along the trajectory and Bader charges; dissociation of the H_2 molecule (PDF)

INCAR files (ZIP)

CIF files (ZIP)

Complete MD trajectory (MP4)

■ AUTHOR INFORMATION

Corresponding Author

*E-mail: rsruoff@ibs.re.kr or ruofflab@gmail.com.

ORCID

Dulce C. Camacho-Mojica: 0000-0002-7932-9655

Feng Ding: 0000-0001-9153-9279

Author Contributions

There are no conflicts to declare. All authors have given approval to the final version of the manuscript.

Notes

The authors declare no competing financial interest.

■ ACKNOWLEDGMENTS

This work was supported by IBS-R019-D1.

■ REFERENCES

(1) Kalantar-Zadeh, K.; Tang, J.; Daeneke, T.; O'Mullane, A. P.; Stewart, L. A.; Lui, J.; Majidi, C.; Ruoff, R. S.; Weiss, P. S.; Dickey, M. D. Emergence of liquid metals in nanotechnology. *ACS Nano* **2019**, *13* (7), 7388−7395.

(2) Dickey, M. D. Strechable and soft electronics using liquid metals. *Adv. Mater.* **2017**, *29*, 1606425.

(3) Wang, K.; Jiang, K.; Chung, B.; Ouchi, T.; Burke, P. J.; Boysen, D. A.; Bradwell, D. J.; Kim, H.; Muecke, U.; Sadoway, D. R. Lithium-antimony-lead liquid metal battery for grid-level energy storage. *Nature* **2014**, *514*, 348−350.

(4) Fujita, J. I.; Hiyama, T.; Hirukawa, A.; Kondo, T.; Nakamura, J.; Ito, S. I.; Araki, R.; Ito, Y.; Takeguchi, M.; Pai, W. W. Near room temperature chemical vapor deposition of graphene with diluted methane and molten gallium catalyst. *Sci. Rep.* **2017**, *7*, 12371.

(5) Shafiei, M.; Hoshyargar, F.; Motta, N.; O'Mullane, A. P. Utilizing p-type native oxide on liquid metal microdroplets for low temperature gas sensing. *Mater. Des.* **2017**, *122*, 288−295.

(6) Zhang, W.; Srichan, N.; Chrimes, A. F.; Taylor, A. F.; Berean, K. J.; Ou, J. Z.; Daeneke, T.; O'Mullane, A. P.; Bryant, G.; Kalantar-Zadeh, K. Sonication synthesis of micro-sized silver nanoparticle/oleic acid liquid marbles: A novel SERS sensing platform. *Sens. Actuators, B* **2016**, *223*, 52−58.

(7) Bobev, S.; Merz, J.; Lima, A.; Fritsch, V.; Thompson, J. D.; Sarrao, J. L.; Gillessen, M.; Dronskowski, R. Unusual Mn-Mn spin coupling in the polar intermetallic compounds $CaMn_2Sb_2$ and $SrMn_2Sb_2$. *Inorg. Chem.* **2006**, *45*, 4047−4054.

(8) Sebastian, C. P.; Malliakas, C. D.; Chondroudi, M.; Schellenberg, I.; Rayaprol, S.; Hoffmann, R. D.; Pottgen, R.; Kanatzidis, M. G.

Indium flux-growth of Eu_2AuGe_3: A new germanide with an AlB_2 superstructure. *Inorg. Chem.* **2010**, *49* (20), 9574−9580.
(9) Daeneke, T.; Khoshmanesh, K.; Mahmood, N.; de Castro, I. A.; Esrafilzedeh, D.; Barrow, S. J.; Dickey, M. D.; Kalantar-Zadeh, K. Liquid metals: fundamentals and applications in chemistry. *Chem. Soc. Rev.* **2018**, *47*, 4073−4111.
(10) Chandler, J. E.; Messer, H. H.; Ellendser, G. Cytotoxicity of gallium and indium ions compared with mercuric ion. *J. Dent. Res.* **1994**, *73* (9), 1554−1559.
(11) Yu, S.; Kaviany, M. Electrical, thermal, and species transport properties of liquid eutectic in Ga-In and Ga-In-Sn from first principles. *J. Chem. Phys.* **2014**, *140* (6), 064303.
(12) Zavabeti, A.; Zhang, B. Y.; de Castro, I. A.; Ou, J. Z.; Carey, B. J.; Mohuiddin, M.; Datta, R. S.; Xu, C.; Mouritz, A. P.; McConville, C. F.; et al. Green synthesis of low dimensional aluminium oxide using liquid metal reaction media: Ultrahigh flux membranes. *Adv. Funct. Mater.* **2018**, *28*, 1804057.
(13) Esrafilzadeh, D.; Zavabeti, A.; Jalili, R.; Atkin, P.; Choi, J.; Carey, B. J.; Brkljaca, R.; O'Mullane, A. P.; Dickey, M. D.; Officer, D. L.; MacFarlane, D. R.; Daeneke, T.; Kalantar-Zadeh, K.; et al. Room temperature CO_2 reduction to solid carbon species on liquid metals featuring atomically thin ceria interfaces. *Nat. Commun.* **2019**, *10*, 865.
(14) Bauer, T.; Maisel, S.; Blaumieser, D.; Vecchietti, J.; Taccardi, N.; Wasserchierd, P.; Bonivardi, A.; Gorling, A.; Libuda, J. Operando DRIFTS and DFT study of propane dehydrogenation over solid − and liquid -supported Ga_xPt_y Catalyst. *ACS Catal.* **2019**, *9* (4), 2842−2853.
(15) Upham, D. Ch.; Agarwal, V.; Khechfe, A.; Snodgrass, Z. R.; Gordon, M. J.; Metiu, H.; McFarland, E. W. Catalytic molten metals for the direct conversion of methane to hydrogen and separable carbon. *Science* **2017**, *358* (6365), 917−921.
(16) Yen, P. S.; Deveau, N. D.; Datta, R. Sandwiched liquid metal membrane (SLiMM) for hydrogen purification. *AIChE J.* **2017**, *63* (5), 1483−1488.
(17) Yen, P. S.; Deveau, N. D.; Datta, R. Dissociative adsorption, dissolution, and diffusion of hydrogen in liquid metal membranes. A phenomenological model. *Ind. Eng. Chem. Res.* **2018**, *57* (5), 1607−1620.
(18) Hohenberg, P.; Kohn, W. Inhomogeneous electron gas. *Phys. Rev.* **1964**, *136*, B864.
(19) Kohn, W.; Sham, L. J. Self-consistent equations including exchange and correlation effects. *Phys. Rev.* **1965**, *140*, A1133.
(20) Kresse, G.; Furthmüller, J. Efficient iterative schemes for ab initio total-energy calculations using a plane-wave basis se. *Phys. Rev. B: Condens. Matter Mater. Phys.* **1996**, *54*, 11169−11186.
(21) Kresse, G.; Furthmüller, J. Efficiency of ab-initio total energy calculations for metals and semiconductors using a plane-wave basis set. *Comput. Mater. Sci.* **1996**, *6*, 15−50.
(22) Henkelman, G.; Arnaldsoon, A.; Jónsson, H. A fast and robust algorithm for Bader decomposition of charge density. *Comput. Mater. Sci.* **2006**, *36*, 354−360.
(23) Yu, M.; Trinkle, D. R Accurate and efficient algorithm for Bader charge integration. *J. Chem. Phys.* **2011**, *134*, 064111.
(24) Alcock, C. B.; Itkin, V. P.; Horrigan, M. K. Vapourpressure equations for the metallic elements: 298 − 2500 K. *Can. Metall. Q.* **1984**, *23* (3), 309−313.
(25) Bader, R. F.W.; Keaveny, I.; Cade, P. E. Molecular charge distributions and chemical binding. 2. First-row diatomic hydrides AH. *J. Chem. Phys.* **1967**, *47* (9), 3381−3402.
(26) Cade, P. E.; Bader, R. F. W.; Henneker, W. H.; Keaveny, I. Molecular charge distributions and chemical binding. IV. Second-raw diatonic hydrides AH. *J. Chem. Phys.* **1969**, *50* (12), 5313−5333.
(27) Politzer, P.; Cusachs, L. C. On the electronic density distribution in diborane. *Chem. Phys. Lett.* **1968**, *2* (1), 1−4.
(28) Downs, A. J.; Goode, M. J.; Pulhan, C. T. Gallane at last! *J. Am. Chem. Soc.* **1989**, *111* (5), 1936−1937.
(29) Pulham, C. R.; Downs, A. J.; Goode, M. J.; Rankin, D. W. H.; Roberson, H. E. Gallane: synthesis, physical and chemical properties, and structure of the gaseous molecule Ga_2H_6 as determined by electron diffraction. *J. Am. Chem. Soc.* **1991**, *113*, 5149−5162.
(30) Laszlo, P. A. Diborane Story. *Angew. Chem., Int. Ed.* **2000**, *39* (12), 2071−2072.
(31) Kuchitsu, K. Comparison of molecular structures determined by electron diffraction and spectroscopy. ethane and diborane. *J. Chem. Phys.* **1968**, *49*, 4456−4462.
(32) Downs, A. J.; Greene, T. M.; Johnsen, E.; Pulham, C. R.; Robertson, H. E.; Wann, D. A. The digallane molecule, Ga_2H_6: experimental update giving an improved structure and estimate of the enthalpy change for the reaction $Ga_2H_6(g)$ -> $2GaH_3(g)$. *Dalton Trans* **2010**, *39*, 5637−5642.
(33) Wei, S.; Oyanagi, H.; Lui, W.; Hu, T.; Yin, S.; Bian, G. Local structure of liquid gallium studied by X-ray absorption fine structure. *J. Non-Cryst. Solids* **2000**, *275* (3), 160−168.
(34) Slater, J. C. Atomic radii in crystals. *J. Chem. Phys.* **1964**, *41*, 3199−3204.
(35) Shannon, R. D. Revised effective ionic radii and systematic studies of interatomic distances in halides and chalcogenides. *Acta Crystallogr., Sect. A: Cryst. Phys., Diffr., Theor. Gen. Crystallogr.* **1976**, *A32*, 751−767.
(36) Gong, X. G.; Chiarotti, G. L.; Parrinello, M.; Tosatti, E. α-gallium: A metallic molecular crystal. *Phys. Rev. B: Condens. Matter Mater. Phys.* **1991**, *43* (17), 14277−14280.

DOI: 10.1021/acs.jpcc.9b06779
J. Phys. Chem. C 2019, 123, 26769−26776